

## Fog Modification with Giant Hygroscopic Nuclei<sup>1</sup>

J. E. JUSTO<sup>2</sup>, R. J. PILIÉ AND W. C. KOCCOND

*Cornell Aeronautical Laboratory, Inc., Buffalo, N. Y.*

(Manuscript received 13 February 1968, in revised form 22 May 1968)

### ABSTRACT

Analytic and experimental investigations were conducted to examine the concept of modifying fog with hygroscopic material. An approximate equation was derived that is useful in estimating the feasibility of such applied problems. The combined results show that it is possible to improve visibility in warm fog by seeding with micron-size salt particles (NaCl). The visibility in laboratory fog produced in a 600-m<sup>3</sup> chamber was increased by factors of 3–10, with as little as 1.7 mg m<sup>-3</sup> of NaCl being effective. Only a modest reduction (<1%) in ambient relative humidity by the giant salt particles is necessary to cause substantial evaporation of the fog droplets. Extrapolation of these results suggests that clearing a suitable landing zone for aircraft should not involve prohibitive amounts of properly sized seeding material.

### 1. Introduction

Despite improved aircraft landing aids at airports, the occurrence of fog continues to hamper flight schedules. Cloud ceilings and ground visibilities  $\leq 300$  ft and 0.5 mi can bring air transportation to a standstill. Fog, which is the most common weather phenomenon to produce these conditions, may persist for a few hours to several days. Efforts to achieve a fog dispersal capability have occupied the attention of atmospheric physicists for at least three decades. While the ability to dissipate thin supercooled clouds and fog has now become reality, modification of "warm" fog (i.e., warmer than 0C) on a practical basis has yet to be achieved.

Over the years there has been periodic interest in the possibility of modifying fogs with hygroscopic materials. The usual intent has been to extract a portion of the water vapor from the saturated air so that evaporation of the fog droplets can occur. The most notable and rigorous effort of this type—and one that achieved limited success—was performed by Houghton and Radford (1938). In their now classic work, clearing of modest size volumes (up to 10<sup>6</sup> m<sup>3</sup>) was obtained by seeding with droplets of calcium chloride solution. The experiments were designed to reduce the ambient relative humidity to approximately 90% with clearing rates of 2000 m<sup>3</sup> sec<sup>-1</sup>. In general, solution spray rates of about 5 liters sec<sup>-1</sup>, or approximately 2.5 gm of seeding material per cubic meter of fog, yielded the desired result.

Our approach has differed from the above in two respects: 1) dry salt particles (sodium chloride) of prescribed sizes are employed, and 2) only slight reductions in ambient relative humidity are demanded, sufficient to alter the droplet size distribution, enhance fallout, and improve visibility above critical landing limits (Pilié *et al.*, 1967).

Means of generating fairly uniform sizes of NaCl nu-

clei—an essential capability—were developed on a laboratory scale. It was hoped that an environmental relative humidity decrease of only 1% or less would still foster significant visibility improvement but not necessitate the marginally large seeding requirements for more rapid fog evaporation. This hypothesis was tested both analytically and experimentally.

### 2. Physical principles

#### a. Visibility factors and objectives

In principle, improvements in fog visibility can be effected by shifting the droplet size distribution to larger sizes and fewer drops, or by decreasing the liquid water content of the fog. These conclusions can be drawn from a form of the visibility equation derived by Trabert (1901), i.e.,

$$V = \frac{C \sum N_i r_i^3}{\omega \sum N_i r_i^2} \approx 2.6 \frac{\bar{r}}{k}, \quad (1)$$

where  $V$  is the visibility in a cloud,  $N_i$  the concentration of droplets of radius  $r_i$ ,  $\omega$  the liquid water content,  $C$  a numerical scattering factor (2.6),  $\bar{r}$  the linear-mean droplet radius, and  $k$  an empirical value (1–2, typically), varying with the width of the droplet size distribution.

Coastal fogs, for example, characteristically possess better visibilities than inland fogs, primarily because of their respective droplet size distribution characteristics (despite the fact that coastal fogs have somewhat higher water content). Hence, modification concepts that show promise of altering droplet size distributions are appealing. Techniques that also incorporate the potential for decreasing fog water content are, of course, most advantageous.

As stated, hygroscopic particles introduced into fog can lower the ambient vapor pressure sufficiently to cause evaporation of natural fog droplets. If submicron particles are used for seeding, the resultant drops will be undesirably small, often leading to increased scat-

<sup>1</sup> Research sponsored by the Aeronautical Vehicles Division, NASA Contract NASr-156.

<sup>2</sup> Present affiliation: State University of New York at Albany.

tered light and even poorer visibility. On the other hand, if excessively large particles are introduced into the fog, more favorable light scattering may be obtained but salt mass requirements soon render the scheme inefficient. Some of the key questions that had to be answered to evaluate the concept were:

1) What are the rates of growth of giant hygroscopic nuclei and the fall times through given depths of fog?

2) What are the optimum sizes of dry salt nuclei in terms of dwell time in the fog, water absorbed per particle, and mass seeding requirements?

3) If only fractional ( $\leq 1\%$ ) reductions in relative humidity are obtained, will evaporation of the natural fog drops be sufficient to improve visibility?

#### b. Droplet growth vs fall distance and time

An approximate expression was derived for the size achieved by giant hygroscopic particles after falling through a given depth of fog and the fall time involved. Essentially, this involves combining three equations: a form of the equation for droplet growth by diffusion, the general velocity equation, and Stokes expression for the terminal velocity of spheres.

The droplet growth equation employed is that given by Fletcher (1962), i.e.,

$$r \frac{dr}{dt} = G \left( S - \frac{a}{r} + \frac{b}{r^3} \right), \quad (2)$$

where  $r$  is droplet radius. The right-hand side of the equation accounts for condensational heating  $G$ , environmental supersaturation  $S$ , Kelvin curvature effect  $a/r$ , and nucleus solubility  $b/r^3$ , all symbols being defined in the Appendix. This expression was simplified by ignoring the curvature effect and taking supersaturation  $S = 0$  (100% relative humidity). Both steps are reasonable in the given fog situation because, with giant hygroscopic nuclei, the solubility term  $b/r^3$  dominates the droplet growth process for substantial periods of time. For example, even after drop size has increased by an order of magnitude on a  $5 \mu$  radius salt nucleus, the Kelvin term is only 2% of the solubility term (approximately 7% after a ten-fold enlargement of a  $1 \mu$  radius nucleus). Should the drops approach their diluted equilibrium sizes, then the simplification is no longer justified. Thus, (2) reduces to

$$dt = r^4 dr / (Gb). \quad (3)$$

The Stokes equation for the velocity  $v$  of falling spheres and the generalized velocity equation used are, respectively,

$$v = \frac{2}{9} \frac{(\rho_0 - \rho a)}{\eta} \approx \frac{2}{9} \frac{\rho_0 g r^2}{\eta}, \quad (4)$$

$$dh = v dt. \quad (5)$$

Substituting Eqs. (3) and (4) into (5) and integrating yields the size  $r_H$  achieved by droplets growing on nuclei

of characteristic  $b$  after falling distance  $H$  in a fog at 100% relative humidity, i.e.,

$$H = \frac{2}{63} \frac{\rho_0 g}{\eta G b} (r_H^7 - r_0^7), \quad (6)$$

$$b = 4.3 i \frac{m_s}{M}, \quad (7)$$

where salt nucleus mass and molecular weight are given by  $m_s$  and  $M$ , and  $i$  is the Van't Hoff dissociation factor.

For sodium chloride particles,  $b \approx 0.147 m_s$ . Assuming further that temperature  $T = 20^\circ\text{C}$ , saline drop density  $\rho_0 = 1.1 \text{ gm cm}^{-3}$ , and initial drop size  $r_0 \ll r_H$ , the general equation (6) may be written as

$$r_H = 192 (m_s H)^{1/7}, \quad (8)$$

for conditions characteristic of our laboratory experiments. From equation (3),

$$t_H = 1.11 \times 10^{-14} r_H^5 / m_s. \quad (9)$$

Thus, Eqs. (8) and (9) yield the resultant size and dwell time of giant salt particles of given mass injected into fogs under the stipulated conditions. While lacking in elegance, these simplified equations permit sound first approximations of fog seeding effects and requirements without the necessity of a computer.

#### c. Seeding model

Calculations of salt-seeding requirements were made in preparation for fog experiments conducted in a 600-m<sup>3</sup> test chamber (described in a subsequent section). The model fog and seeding conditions assumed were as follows:

- Fog depth  $H = 10$  m (height of facility)
- Temperature, 20C
- Saturation vapor density, 18 gm m<sup>-3</sup>
- Natural fog drop radii, 5  $\mu$
- Initial fog liquid water content, 0.2 gm m<sup>-3</sup>
- Salt (NaCl) injected at top of fog

Invoking the above conditions and employing Eqs. (8) and (9), the final drop size and fall time of droplets in the chamber were calculated as a function of salt nucleus size. It is a straightforward matter to compute the mass of water extracted per giant nucleus and the total concentration and amount of salt needed to fulfill the indicated clearing objective, i.e., to absorb 0.2 gm m<sup>-3</sup> of fog water. This degree of seeding may be thought of as that just sufficient to evaporate the natural fog droplets and to transfer the vapor to the absorbing salt particles in the times shown. The resulting estimates are shown in Table 1.

An idealized estimate of maximum visibility improvement that can be obtained solely by shifting the drop-size distribution is shown in the last column of Table 1. These values result from application of the Trabert visibility formula [Eq. (1)] and the simplifying assump-

TABLE 1. Droplet growth and fog seeding requirements for laboratory model fog.\*

Salt particle		Final drop size $r_H$ ( $\mu$ )	Fall time $t_H$ (sec)	Water per particle $m_p$ ( $10^{-8}$ gm)	Required salt conc. ( $\text{cm}^{-3}$ )	Required salt mass ( $\text{mg m}^{-3}$ )	Visibility improvement factor
Radius ( $\mu$ )	Mass (gm)						
47.8	$10^{-6}$	71.5	21	54.0	0.37	370	14
22.4	$10^{-7}$	51.5	40	47.4	0.42	42	10
10.0	$10^{-8}$	36.8	76	19.9	1.0	10.0	7
4.78	$10^{-9}$	26.3	141	7.60	2.6	2.7	5
2.24	$10^{-10}$	18.9	270	2.84	7.0	0.70	3.5
1.0	$10^{-11}$	13.7	536	1.08	18.5	0.18	2.5

\* Model fog  $T=20\text{C}$ ; fog depth, 10 m;  $\text{LWC}=0.2 \text{ gm m}^{-3}$ ; drop radii,  $5 \mu$ ; RH, 100%; water absorbed by salt,  $0.2 \text{ gm m}^{-3}$ .

tion of monodisperse drop sizes, i.e., the initial model-fog drops are replaced by larger but fewer saline drops of the size shown in column 3 after appropriate seeding. Since total liquid water is quasi-constant, the visibility improvement factor is merely the final drop radius divided by the initial fog-drop radius ( $5 \mu$ ). For example,  $2.2 \mu$  radius salt nuclei introduced into the fog in concentrations of  $7 \text{ cm}^{-3}$  ( $0.42 \text{ gm total}$ ) should grow to  $18.9 \mu$  radius droplets during their residence time. This corresponds to a visibility improvement factor of about 3.5. After 270 sec, the drops then settle out and further improvement in visibility is to be expected.

Slight temperature effects due to the heat of solution of the NaCl, heat of condensation of water vapor on the salt nuclei, and cooling resulting from evaporation of natural fog drops were ignored. Owing to the small mass of salt and the slight humidity reductions involved, these modest temperature variations are of secondary importance.

The following conclusions can be drawn from the data presented in Table 1:

1) As salt particle size decreases, the total payload required to absorb  $0.2 \text{ gm m}^{-3}$  of fog liquid water steadily decreases. Particle fall time in the 10-m high fog undergoes a corresponding increase, with salt nuclei  $< 1 \mu$  radius being generally impractical.

2) From the Trabert visibility equation, it is apparent that the larger nuclei lead to bigger (fewer) drops and better visibilities. Initially, when liquid water content is essentially constant, the visibility improvement is directly proportional to the final drop size achieved. However, the choice of larger particle size is not unlimited as payloads go up significantly.

3) The optimum salt particle radius, considering final drop size, fall time and total required mass, is approximately  $5 \mu$ . An acceptable size range appears to be from 2–10  $\mu$  radius under saturated conditions.

If more salt particles are used in order to reduce the ambient relative humidity and to speed evaporation, saline-drop growth will decrease and particle dwell time increase. Eq. (2) then should be used to determine the salt requirement under these more involved conditions. Such numerical tabulations (Justo, 1967) show that to decrease the ambient relative humidity by 1%, the salt

requirement of 5–10  $\mu$  radius particles must be increased by about a factor of 3. (The factor is about 30 if a relative humidity of 96% is the objective.) Particles of  $2 \mu$  radius and less become undesirable as they achieve equilibrium sizes that are ineffectively small. (At 96% even  $5 \mu$  radius nuclei are of limited use.)

Thus "excessive" drying of the environment, while facilitating natural fog droplet evaporation, can stabilize the growth rate of injected giant nuclei and partially impede desired improvements in visibility. This is not critical if appropriately large nuclei are used that fall out of the system in reasonable times, but salt mass requirements increase dramatically.

#### d. Evaporation rate of natural fog droplets

As noted previously, sufficient water vapor must be extracted from the fog air by the giant salt nuclei to allow the natural fog droplets to evaporate. At the slight subsaturations involved (or at 100% relative humidity), will evaporation rates be significant?

Numerical calculations of evaporation rate as a function of ambient relative humidity were made using Eq. (2). It was assumed that the natural fog drops had condensed on typical  $0.1 \mu$  radius nuclei of NaCl. The time required for given size droplets to evaporate, i.e., reach small equilibrium sizes, was determined and the results plotted in Fig. 1.

The speed with which small droplets (typical inland fog sizes shown) evaporate is both revealing and encouraging in terms of the fog seeding objective. The model fog droplets of  $5 \mu$  radius will evaporate in 10 sec at a relative humidity of 99%, 1.3 min at 99.9%, and 6 min at 100%. Hence, substantial drying of the atmosphere, which was shown in the last section to lead to prohibitively large salt masses, does not appear essential. An optimum ambient humidity to strive for, recognizing that such control is not generally possible in practice, is approximately 99.5–99.9%.

### 3. Fog seeding experiments

The primary objectives of fog seeding experiments were: 1) to determine the maximum improvement in visibility that could be achieved by seeding with NaCl nuclei of carefully controlled size, 2) to determine the minimum amount of material required to achieve the

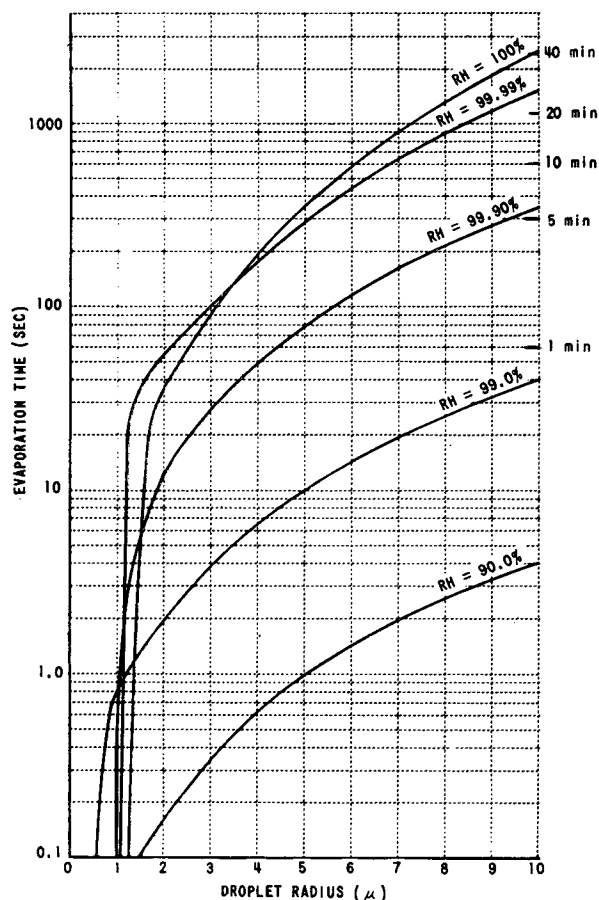


FIG. 1. Evaporation times of droplet vs relative humidity for droplet nuclei consisting of  $0.1 \mu$  radius NaCl particles.

desired visibility improvement, and 3) to compare observed results with theoretical predictions.

The procedure used was to produce one fog for use as a control and to measure its microphysical characteristics as a function of time. A second fog was then produced and seeded with a predetermined mass of NaCl, and comparisons made with the control fog. Two types of fogs were involved—those which were slowly dissipating and those of a persistent nature, i.e., fogs showing no improvement in visibility over approximately a 25-min period.

#### a. Equipment for fog generation

The fog facility, shown in Fig. 2, consists of a cylindrical chamber which can be pressurized or evacuated at controlled rates. In essence, quasi-adiabatic expansions are produced, and under appropriate humidity conditions, fogs form. These laboratory fogs were found to possess liquid water contents and drop-size distributions that are representative of natural inland fogs.

The large chamber is 30 ft in diameter and 30 ft high, enclosing a volume of approximately  $600 \text{ m}^3$ . Construction material consists of 0.5-inch sheet steel with an epoxied inner surface. As shown, a rotating spray nozzle

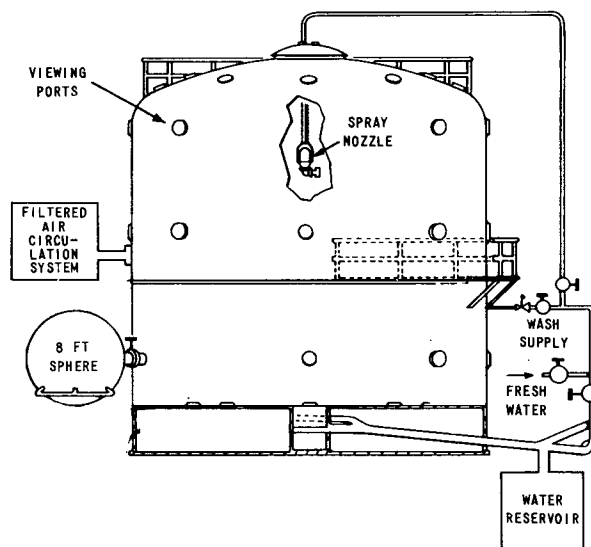


FIG. 2. The  $600\text{-m}^3$  test chamber at Ashford, N. Y.

enables the walls and floor of the chamber to be thoroughly wetted with water, and the relative humidity of the air to approach 100%. Glass ports are located at various levels for monitoring the fog visually or with transmissometers. Ports in the domed ceiling allow convenient dispersal of seeding material.

By means of a blower-circulation system, the chamber is pressurized to approximately 20 cm of water. After permitting the internal temperature and humidity to equilibrate with the wet walls, the chamber is vented to the outside at controlled rates. Alternately, air can be pumped from the large chamber at controlled rates to produce the expansion.

The fogs formed in the above manner slowly decay as the droplets evaporate. Typical working times are approximately 20–25 min. More persistent fogs were generated by initiating a slow secondary expansion following the initial fog-forming expansion. Moreover, fog visibility could be held nearly constant by appropriately regulating the secondary expansion.

#### b. Microphysics equipment

The primary sensors used to monitor fog characteristics were: 1) two transmissometers for determining horizontal visibility (i.e., extinction coefficient) over a 60-ft path (30 ft baseline with reflecting mirror), one transmissometer being located at a 4-ft level, the second at 15 ft; 2) a fog-droplet sampler employing a gelatin replication technique (Justo, 1965) for measuring drop-size distributions during the fog's life cycle; 3) psychrometric equipment for estimating relative humidity at the lower level; 4) temperature sensors arrayed vertically at heights between 4 and 24 ft; and 5) cloud nucleus counter and Aitken counter for monitoring condensation nucleus concentrations.

Transmissometer data and temperature information

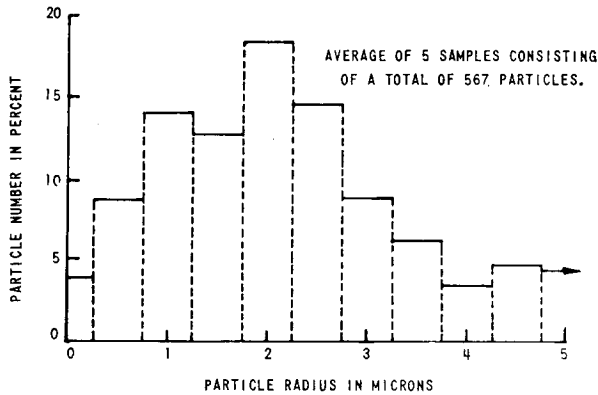


FIG. 3. Size distribution of NaCl nuclei produced by the particle classifier-disseminator used in the fog seeding experiments.

were recorded externally, while the other equipment was manually operated from within the chamber.

A modified Trost Jet Mill<sup>3</sup> was used to classify and disseminate salt nuclei into the chamber during seeding experiments. This mill makes use of two opposing jets of air or bottled gas to grind material. By the addition of a baffle in the centrifuge portion of the unit and a second emission port, it was found that particle sizing could be achieved. Salt was ground and classified with the jet mill and then stored in bottles for subsequent use; during an experiment the mill was used again merely to disperse the pre-classified salt. A typical size distribution of sodium chloride particles is shown in Fig. 3, indicating that approximately 85% of the particles are between 1 and 5  $\mu$  radius.

#### c. Analysis procedures

In order to assess the effects of seeding fogs with hygroscopic nuclei, four microphysical quantities were determined: the extinction coefficient  $\beta$  (or visibility  $V$ ), droplet size distribution, drop concentration  $N$ , and fog liquid water content  $\omega$ . The transmissometer enables measurements of  $\beta$ , the droplet sampler yields size information, and these two instruments combined allow determinations of  $N$  and  $\omega$ . While the latter two quantities, in principle, can be obtained from the droplet slide data alone, greater accuracy is afforded by taking advantage of transmissometer information.

The intensity of light observed with a transmissometer is given by

$$I = I_0 e^{-\beta x}, \quad (10)$$

where  $I_0$  is the intensity observed in clear air, and  $x$  is the length of the transmission path in the fog. Visibility  $V$  is computed from such data according to the Koschmieder (1924) approximation

$$V = 3.912/\beta. \quad (11)$$

For fog conditions, the extinction coefficient is approxi-

<sup>3</sup> Manufactured by Helme Products, Inc., Helmetta, N. J.

mately equal to the Mie scattering coefficient, such that

$$\beta = \sum \pi N_i r_i^2 k_s, \quad (12)$$

where the scattering area coefficient  $k_s$  is taken as 2.

By means of the Trabert expression previously discussed, the liquid water content can be calculated (aufm Kampe and Weickmann, 1957) from

$$\omega = \frac{2.6 \sum N_i r_i^3}{V \sum N_i r_i^2}. \quad (13)$$

In similar fashion it can be shown [by multiplying both sides of Eq. (1) by total droplet concentration  $N$ ] that

$$N = \frac{0.622 \sum N_i}{V \sum N_i r_i^2}. \quad (14)$$

It is estimated that the accuracy of measuring  $\beta$  (and visibility) is about 5%. The uncertainty in droplet distributions is largely a function of the number of droplets counted. Our samples usually consisted of between 200 and 300 droplets. These uncertainties in droplet distributions, particularly of the large drops, result in estimated accuracies for liquid water content and droplet concentration of the order of 25% in seeded fogs, with higher accuracy in control fogs.

#### 4. Fog seeding results

Approximately 20 individual experiments (10 pairs) were conducted. Of the 10 seeding cases, all except one resulted in some significant visibility improvement. In the case where visibility was not improved, a small concentration of salt purposely was used to establish the lower limit on mass requirements.

Typical physical characteristics of the laboratory fogs approximately 1 min after completion of the expansion are shown in Table 2 and compared with representative inland radiation fog characteristics as determined from the literature. It is apparent that fairly realistic fog simulation was achieved.

Table 3 summarizes the visibility improvement (seeded fog relative to control fog) as a function of time after seeding. Visibility improvement factors of 2 to 5 during the test periods involved were not uncommon with greater improvements occasionally noted. For the salt size-distributions involved (approximately 1–5  $\mu$  radii), it is evident from Table 1 calculations that this is the right order of improvement to be expected. Fur-

TABLE 2. Characteristics of laboratory and natural radiation fogs.

Fog parameter	Laboratory fog	Natural radiation fog
Average drop radius	4–5 $\mu$	5 $\mu$
Typical drop radius range	1–22 $\mu$	2–18 $\mu$
Liquid water content	150–200 mg m <sup>-3</sup>	110 mg m <sup>-3</sup>
Droplet concentration	250–500 cm <sup>-3</sup>	200 cm <sup>-3</sup>
Visibility	200–400 ft	300–900ft

TABLE 3. Visibility improvement factors\* for seeding experiments.

Seeding mass (mg m <sup>-3</sup> )	Time from start of seeding				
	4 min	8min	12 min		
<i>Normal laboratory fog</i>					
51	1.6; 0	10; 4.9	2.4; 3.9		
51	1.5; 0	5.7; 1.6	3.6; 6.7		
8	1.8; 5.1	5.0; 9.1	1.1; 2.9		
4	1.4; 2.3	7.6; 9.4	1.8; 1.6		
1.6	1.2; 1.2	1.7; 4.0	4.5; 6.7		
0.8	-; 0	0; -1.1	0; -1.1		
<i>Persistent fog</i>					
	4 min	8 min	12 min	16 min	20 min
8	2.4; 1.7	5.2; 2.4	5.0; 3.2	3.6; 3.5	3.5; 2.8

\* Improvement factor is defined as the ratio of the visibility of the seeded fog to the visibility of the control fog at the same time after initiation of the expansion: first tabular entry at 15-ft level; second at 4-ft level.

ther, the observed lower bound on effective salt mass (between 0.8 and 1.7 mg m<sup>-3</sup>) is quite consistent with theoretical expectations.

Applying the analytical predictions of Table 1 to the actual salt particle distributions generated (Fig. 3), one can compute weighted mean values of the visibility improvement factor and of the salt mass required. The calculated mean values are a visibility improvement factor of 3.3 and a minimum salt requirement of 0.83 mg m<sup>-3</sup>. Thus, recognizing the limitations in experimentally duplicating the idealized conditions of Table 1, close agreement between theory and observation was indicated.

Results of a persistent fog experiment are shown in Fig. 4. The solid and dashed curves show fog visibility as a function of time for control and seeded fogs, respectively. A salt concentration of 8 mg m<sup>-3</sup> was employed in the seeded case. It is noteworthy that even though the secondary expansion caused rather extreme cooling (4C hr<sup>-1</sup>), visibility improvement factors of 2-3 at the lower level and as much as 5 at the 15-ft level were achieved.

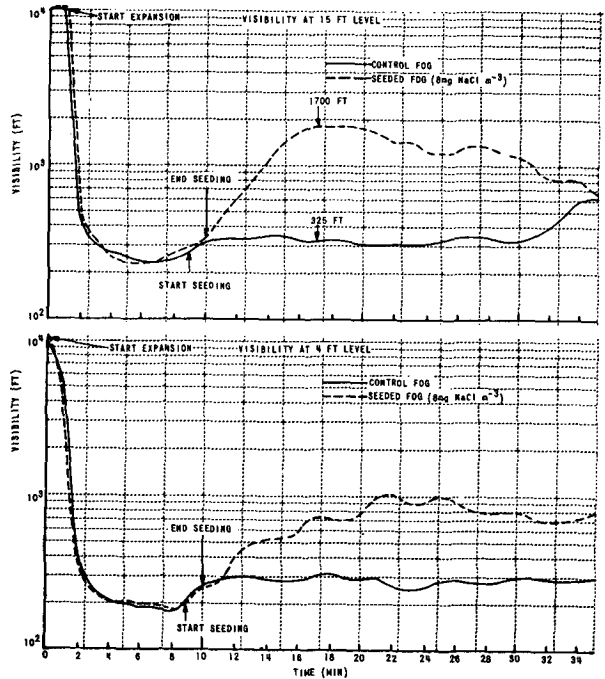


FIG. 4. Visibility as a function of time for a seeded and control fog.

Droplet samples, illustrated in Fig. 5a, were obtained on gelatin-coated slides (2 mm wide) that were automatically exposed to the fog at droplet impact velocities of approximately 30 m sec<sup>-1</sup>. Corresponding dropsize distributions, after applying collection efficiency corrections, are shown in Fig. 5b.

Figs. 6 and 7 depict visibility and fog characteristics as a function of time in two representative fog-seeding cases. The second portion of each of these figures shows the ratio of visibility improvement, seeded to control fogs, and the respective contribution to increased visibility due to induced changes in the dropsize distribu-

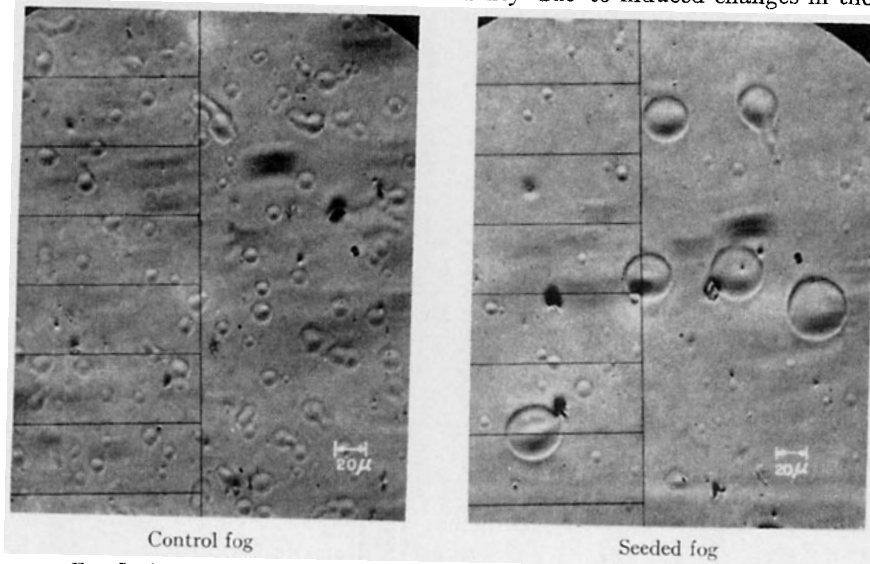


FIG. 5a. Droplet impressions obtained at 8 min in the persistent fog experiment.

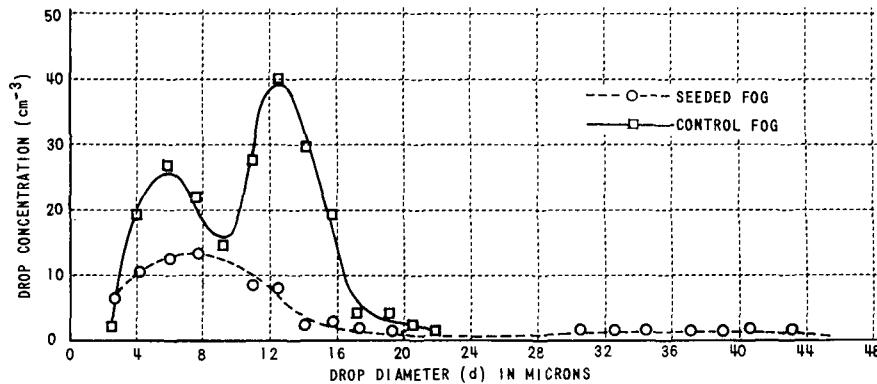


FIG. 5b. Dropsizes distributions for seeded and unseeded fogs at 8 min in the persistent fog experiment.

tion and liquid water content of the fog. The first portions of each figure show fog droplet spectra at selected times, while droplet concentration and liquid water content calculated from Eqs. (13) and (14) are plotted in the lower half of the figures.

For example, at  $t=11$  min in Fig. 6, a factor of 5 improvement in visibility of the seeded fog over the control fog is evident. The five-fold improvement can be accounted for by liquid water content differences (a factor of 1.5) and changes in dropsizes distribution (a factor of 3.3 improvement). At this time, the droplet concentrations in seeded and control fogs were  $6 \text{ cm}^{-3}$  and  $220 \text{ cm}^{-3}$ , respectively. Hence, seeding had the hoped-for effect of shifting the dropsizes distribution so as to form larger but fewer drops, with an attendant decrease in liquid water content.

The case histories shown in Fig. 7 were obtained in the persistent fog experiment in which a secondary expansion was maintained. The transmissometer data and the droplet sample data indicate that the seeded and control fogs at the 4-ft level were essentially identical up to  $t=3$  min, with both liquid water contents being quite similar,  $0.19$  and  $0.20 \text{ gm m}^{-3}$ . The trend of the data indicates that LWC of the control fog increased from  $0.18$  to  $0.28 \text{ gm m}^{-3}$  over the period from 3–20 min. The increase in LWC is undoubtedly the result of droplet growth due to the secondary expansion. Visibility throughout this period remained essentially constant at 300 ft (see Fig. 4).

In the seeded fog, it appears that there was a slight increase in LWC between 4 and 8 min, followed by a return to the initial value at 12 min and a continued decrease to about  $0.12 \text{ gm m}^{-3}$  at 20 min. This sequence is consistent with expectations, i.e., water vapor should condense rapidly on the salt particles for the first few minutes after they are introduced, thereby increasing LWC; later, as these particles grow, they begin to fall out and remove water from the fog.

At 12 min, the visibility of the seeded fog was 2.7 times better than that of the control fog, a factor mainly attributable to the change in dropsizes distribution. While this value is somewhat smaller than the improvement expected from the calculations of Table 1, the

difference is attributable to the increased water made available by the secondary expansion.

Visibility increased to a value of 950 feet at 16 min, a three-fold improvement over the initial value. Of this, an improvement factor of 1.6 was associated with the dropsizes distribution change and a factor of 2.0 associated with the decrease in LWC. Visibility dropped to approximately 800 ft at 20 min and remained in this vicinity until the end of the experiment at 27 min. Analysis of the last droplet sample at 20 min indicates that the net improvement in visibility at that time was due predominantly to a LWC reduction.

In summary, the processes that caused the improvement of visibility of the seeded fog relative to the control fog behaved in a consistent and logical manner during the experiment. During the first 8–10 min after seeding, the shift in dropsizes distributions caused virtually the entire visibility improvement. From that time on, a reduction in liquid water content of the seeded fog, due to the precipitation of water condensed on the larger salt nuclei, became increasingly important; ultimately it was the dominant factor. Obviously, salt seeding served to lower ambient humidity sufficiently to evaporate many of the natural fog droplets (note the reduction in droplet concentrations).

## 5. Hypothetical fog modification at airports

The foregoing analysis was extended to obtain an estimate of the requirements and feasibility of clearing a hypothetical airport fog. The fog volume considered was  $10^8 \text{ m}^3$ , equivalent to a zone 500 m wide, 100 m high, and 2000 m long. Model fog conditions, except for height (now 100 m high), were as stipulated previously (Section 2c).

The seeding effects and requirements are indicated in Table 4. Again,  $5 \mu$  radius salt nuclei appear optimum. As such, 90 kg of material are required for one seeding, in which case an initial (idealized) visibility improvement factor upwards of 7 prior to fallout might be achieved. With a  $3 \text{ m sec}^{-1}$  wind speed, about 5 such seedings per hour or  $450 \text{ kg hr}^{-1}$  would be required for continuous airport operation. Should faster particle fall

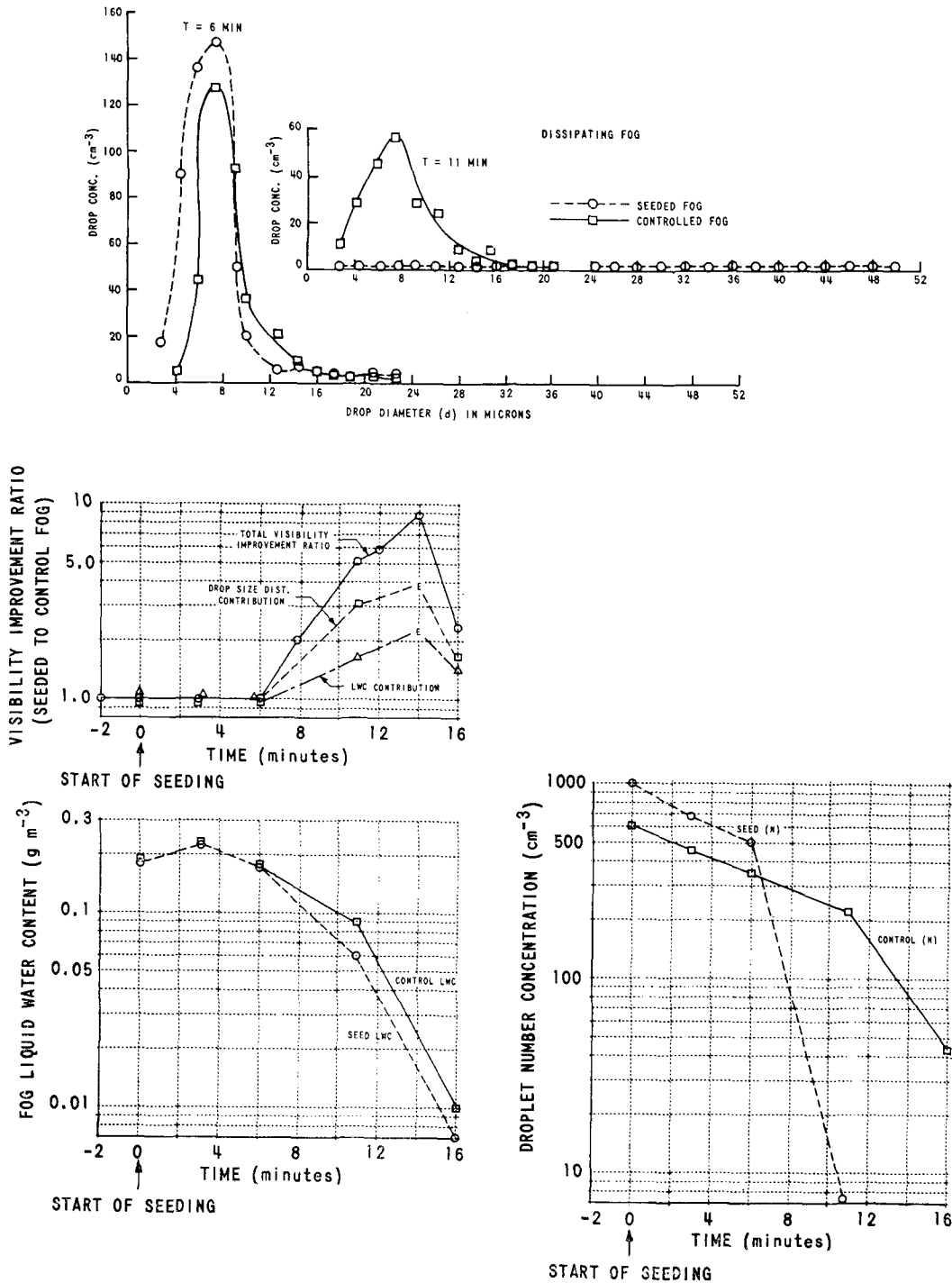


FIG. 6. Fog seeding results in dissipating laboratory fogs using  $4 \text{ mg m}^{-3}$  NaCl seeding mass. (See text for discussion.)

times prove necessary, the use of say  $10 \mu$  radius nuclei would dictate corresponding seeding rates of  $1600 \text{ kg hr}^{-1}$ . The concept might then be testing the limit of feasibility. [It is of interest to note that on a comparable fog volume basis, this latter requirement is still over 2 orders of magnitude lower than that required by Houghton and Radford (1938) to decrease fog humidity to 90%.]

It should be emphasized that the foregoing values are first-order estimates subject to further refinement and field verification. Complicating factors such as particle size variations, inhomogeneities in atmospheric salt distribution, complex heating and cooling effects, and turbulent diffusion will all influence field applications. Nevertheless, a reasonable understanding of the processes involved in the laboratory situation has been ob-



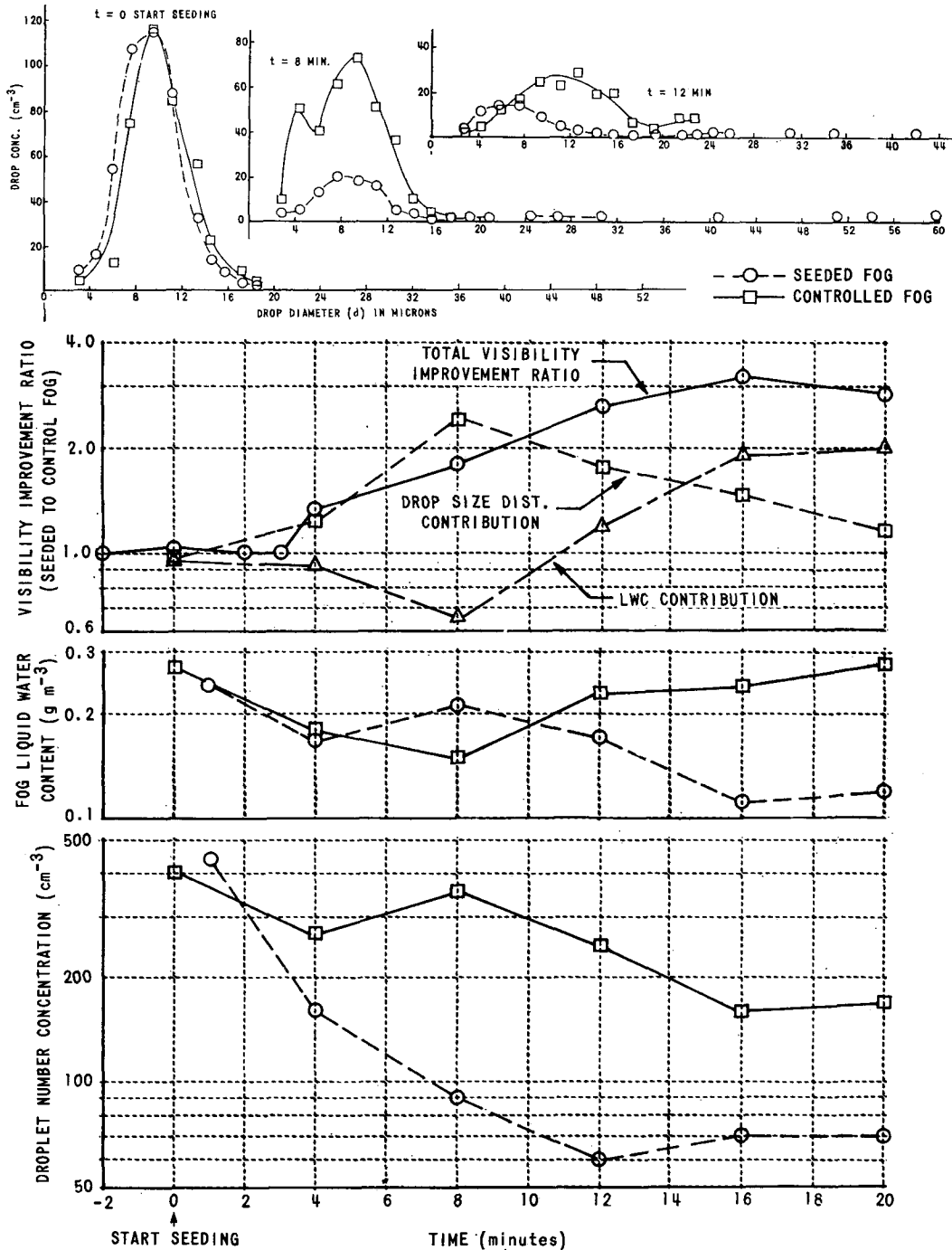


FIG. 7. Fog seeding results in a persistent laboratory fog using  $8 \text{ mg m}^{-2}$  NaCl seeding mass. (See text for discussion.)

tained such that the next logical step, field experimentation, is warranted.

6. Conclusions

The conclusion drawn from this investigation is that fog seeding procedures, in which carefully controlled sizes and amounts of hygroscopic (NaCl) nuclei are

used, can produce significant improvements in the visibility of fog. Two processes are responsible: an initial improvement in visibility results from a change in drop-size distribution from a fog consisting of a large concentration of small droplets to one consisting of a small concentration of large drops. In short, the saline drops grow at the expense of the evaporating natural fog droplets. This change in distribution is accompanied by

TABLE 4. Hypothetical fog clearance at an airport.\*

Salt particle		Final drop size	Fall time	Water per particle	Required salt conc.	Required salt mass for
Radius ( $\mu$ )	Mass (gm)	$r_H$ ( $\mu$ )	$t_H$ (sec)	( $10^{-8}$ gm) $m_p$	( $\text{cm}^{-3}$ )	( $10^8 \text{ m}^3$ ) (kg)
47.8	$10^{-6}$	99.3	110	206	0.098	9720
22.4	$10^{-7}$	71.6	210	179	0.112	1120
10.0	$10^{-8}$	51.1	390	61.5	0.325	325
4.78	$10^{-9}$	36.5	730	22.2	0.901	90
2.24	$10^{-10}$	26.3	1400	8.36	2.39	24
1.0	$10^{-11}$	19.0	2780	3.17	6.31	6.3

\* Model fog  $T=20\text{C}$ ; fog depth, 100 m; LWC= $0.2 \text{ gm m}^{-3}$ ; drop radii,  $5 \mu$ ; RH, 100%; water absorbed by salt,  $0.2 \text{ gm m}^{-3}$ .

a decrease in extinction coefficient, at first without significantly altering the liquid water content. As time progresses, precipitation of droplets will result in additional improvement in visibility.

Effective fog clearance with hygroscopic nuclei entails many considerations and compromises between required payloads, dropsizes, and fall times of particles. Calculations indicated that for typical fogs, salt nuclei of approximately  $5 \mu$  radius in concentrations of 2-3 mg  $\text{m}^{-3}$  are quite favorable. To minimize the required salt mass, it is desirable to seed with just enough material to promote complete evaporation of natural fog droplets and leave the ambient atmosphere near saturation after the evaporation is complete. *A priori* information on fog depth, liquid water content, and wind speed must be considered in advance of an operation. The ability to specify and generate salt nuclei of desired sizes is essential.

These factors were considered in the laboratory fog tests, and theory and observation were in good agreement. Whether the free atmosphere, with its added variables, is as accommodating remains to be determined.

*Acknowledgments.* We are indebted to Mr. Vito DePalma for his part in the design and testing of the particle classifier-disseminator; to Mr. Calvin Easterbrook for the design of the transmissometers; to Mr. George Zigrossi for his assistance in maintaining equipment and obtaining the data; and to Mr. Eugene Mack for analyzing much of the data.

APPENDIX

List of Symbols

- a* droplet curvature term ( $3.3 \times 10^{-5} \text{ T}^{-1}$ )
- b* droplet solubility term
- C* Mie scattering factor (2.6)
- D* diffusivity of water
- g* gravitational acceleration
- G* thermodynamic function in drop growth equation

$$G = \frac{D\rho_v}{\rho} \left[ 1 + \frac{DL^2\rho_v}{R_v T^2 \kappa} \right]^{-1}$$

- h, H* height
- i* van't Hoff factor

- I* intensity of light ray after passing through fog
- I<sub>0</sub>* light intensity in clear air
- k* empirical value for droplet spectrum width
- k<sub>s</sub>* scattering area coefficient
- L* latent heat of vaporization of water
- m<sub>s</sub>* mass of hygroscopic nucleus
- M* molecular weight of nucleus
- N* drop concentration per unit volume
- r* droplet radius
- $\bar{r}$  linear-mean droplet radius
- r<sub>0</sub>, r<sub>H</sub>* initial drop radius and final drop radius after falling distance *H*
- RH relative humidity
- S* supersaturation
- t* time
- R<sub>v</sub>* gas content for water vapor
- T* temperature
- V* visibility
- v* velocity
- x* path length
- $\beta$  extinction coefficient
- $\kappa$  thermal conductivity of air
- $\rho$  density of liquid water
- $\rho_a, \rho_0$  density of air and of drop respectively
- $\rho_v$  saturation water vapor density
- $\eta$  viscosity of air
- $\omega, \text{LWC}$  liquid water content

REFERENCES

aufm Kampe, H. J., and H. K. Weickmann, 1957: Physics of clouds. *Meteor. Mono.*, 3, No. 12-20, 182-226.

Fletcher, N. H., 1962: *The Physics of Rainclouds*. Cambridge University Press, 386 pp.

Houghton, H. G., and W. H. Radford, 1938: On the local dissipation of natural fog. *Papers Phys. Oceanogr. Meteor.*, 6, No. 3, 63 pp.

Justo, J. E., 1965: Cloud particle sampling. Rept. No. 6, NSF G-24850, Dept. of Meteorology, Pennsylvania State University, 19 pp.

—, 1967: Nucleation factors in the development of clouds. Ph.D. dissertation, Dept. of Meteorology, Pennsylvania State University. 124 pp.

Koschmieder, H., 1924: Theorie der horizontalen Sichtweite. *Beitr. Phys. Atmos.*, 12, 33-53.

Pilié, R. J., W. C. Kocmond and J. E. Justo, 1967: Warm fog suppression in large scale laboratory experiments. *Science*, 157, 1319-1320.

Trabert, W., 1901: Die Extinction des Lichtes in einem truben Medium (Schweite in Wolken)., *Meteor. Z.*, 18, 518-520.